Agricultural and Forest Meteorology 150 (2010) 1046–1056

Contents lists available at ScienceDirect

Agricultural and Forest Meteorology

journal homepage: www.elsevier.com/locate/agrformet

A comparison of sap flux density using thermal dissipation, heat pulse velocity and heat field deformation methods

Kathy Steppe[a,*], Dirk J.W. De Pauw[b], Tanya M. Doody[c], Robert O. Teskey[d]

[a] Laboratory of Plant Ecology, Department of Applied Ecology and Environmental Biology, Faculty of Bioscience Engineering, Ghent University, Coupure links 653, B-9000 Ghent, Belgium
[b] Phyto-IT, Beekstraat 23/B, B-9030 Mariakerke, Belgium
[c] CSIRO, PMB 2, Glen Osmond, 5064 South Australia, Australia
[d] Warnell School of Forestry and Natural Resources, University of Georgia, Athens, GA 30602, USA

ARTICLE INFO

Article history:
Received 6 October 2009
Received in revised form 10 February 2010
Accepted 7 April 2010

Keywords:
Error analysis
Fagus grandifolia
Radial profile
Sap flow
Sap velocity
Time constant
Transpiration

ABSTRACT

A laboratory test and field evaluation were conducted to determine the accuracy of the three commonly used techniques for measuring sap flux density in trees: heat pulse velocity, thermal dissipation and heat field deformation. In the laboratory test a constant flow rate of water was maintained through freshly cut stem segments of diffuse-porous *Fagus grandifolia* trees with mean sapwood depths of 4.02 ± 0.14 and 7.44 ± 0.51 cm for sample trees with stem diameter at breast height of 15 and 21 cm, respectively. The three sensor types were measured simultaneously and compared against gravimetric measurements. All three techniques substantially underestimated sap flux density. On average the actual sap flux density was underestimated by 35% using heat pulse velocity (with wound correction), 46% using heat field deformation and 60% using thermal dissipation. These results were consistent across sap flux densities ranging from 5 to 80 $cm^3\,cm^{-2}\,h^{-1}$. Heat pulse velocity measurements were more variable than those of the other two techniques, and the least accurate at low sap flux densities. An error analysis was conducted on all parameters of the equations used with each technique. That analysis indicated that each technique has unique sensitivities to errors in parameter estimates which need to be taken into consideration. Except for the use of heat, the three techniques are quite different and there appeared to be no single reason why the methods underestimated actual sap flux density, but rather there were likely multiple errors that compounded to reduce the overall accuracy of each technique. Field measurements supported the relative sensor performance observed in the laboratory. Applying a sensor-specific correction factor based on the laboratory test to the field data produced similar estimates of sap flux density from all three techniques. We conclude that a species-specific calibration is necessary when using any of these techniques to insure that accurate estimates of sap flux density are obtained, at least until a physical basis for an error correction can be proposed.

1. Introduction

Many researchers need accurate estimates of whole-tree water use in order to assess individual tree transpiration, scale to stand- and catchment-level transpiration, or to understand the contribution of trees to total ecosystem transpiration (e.g., Ford et al., 2008; Mitchell et al., 2009). Heat-based sap flow methods, typically used at stem level, allow quantification of whole-tree water use without altering the transpiration conditions (Schurr, 1998; Smith and Allen, 1996). In contrast, estimation of whole-tree water loss using leaf level measurements is cumbersome and nearly impossible due to the need to scale the measurements over the tree canopy, while accounting for its complexity resulting from variations in leaf age, illumination and boundary layer conductance (Ansley et al., 1994; Ford et al., 2004b).

Methods using heat to sense sap movement in the stem xylem have a long history (Swanson, 1994). The earliest attempt dates back to the work of Huber (1932) whose idea was developed further by Huber and Schmidt (1937) and Dixon (1937), but it was Marshall (1958) who conducted the theoretical analysis of these earlier heat transport experiments and measurement configurations and established the basis for the now well-known heat pulse velocity (HPV) technique, in which sap flux density is determined from the velocity of a short pulse of heat moving along xylem tissue through conduction and convection. This was followed by the development of other techniques where, rather than using short pulses of heat,

* Corresponding author at: Laboratory of Plant Ecology, Department of Applied Ecology and Environmental Biology, Faculty of Bioscience Engineering, Ghent University, Coupure Links 653, B-9000 Gent, Belgium. Tel.: +32 9 264 61 12; fax: +32 9 224 44 10.
E-mail addresses: kathy.steppe@UGent.be (K. Steppe), dirk.depauw@phyto-it.com (D.J.W. De Pauw), tanya.doody@csiro.au (T.M. Doody), teskey@warnell.uga.edu (R.O. Teskey).

0168-1923/$ – see front matter © 2010 Elsevier B.V. All rights reserved.
doi:10.1016/j.agrformet.2010.04.004

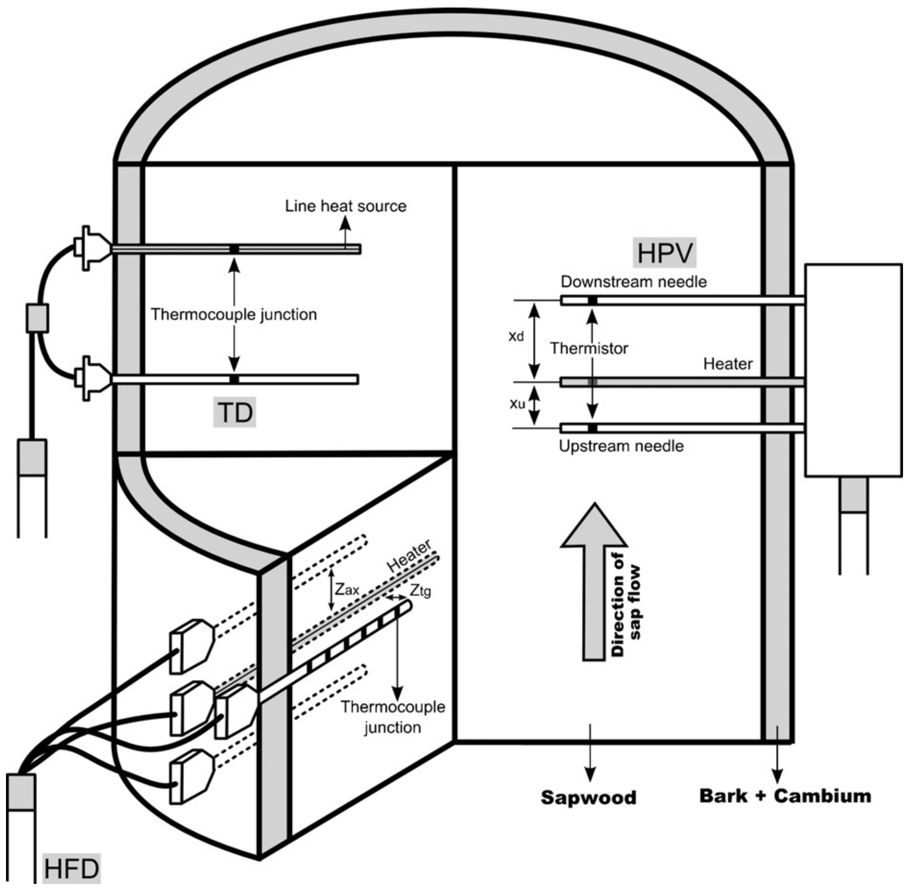

Fig. 1. Schematic diagram of the heat pulse velocity (HPV) sensor, the thermal dissipation (TD) sensor and the heat field deformation (HFD) sensor, installed radially into a stem segment. Symbols: x_d and x_u are the distances between the heater and the downstream and upstream needle of the HPV sensor, respectively; Z_{ax} and Z_{tg} are the distances between the heater and the upper junction of the axial and tangential thermocouple of the HFD sensor, respectively.

continuous heating was applied. Two early attempts used a continuous heat source with temperature sensors arranged around the heater (Viewig and Ziegler, 1960; Ittner, 1968). The latest iteration is the heat field deformation (HFD) method (Nadezhdina et al., 1998). This method records changes in the heat field around a linear heater at different radial positions in the xylem and relates the heat field deformation to sap flux densities in the stem xylem. Another approach is the thermal dissipation (TD) method proposed by Granier (1985) which also uses continuous heating but the temperature is only measured below the heater.

As with all sap-flow techniques, accuracy is a key issue for these three methods. Potential errors in measurement of sap flux density using the well-established TD and HPV techniques and the potential need for species-specific calibration curves have been highlighted in the past (e.g., Green and Clothier, 1988; Swanson, 1994; Smith and Allen, 1996; Clearwater et al., 1999). However, a validation of the relatively new HFD technique is lacking and a simultaneous evaluation of TD, HPV and HFD against gravimetric measurements in tree stems has not been performed. The main objective of this study was therefore to determine whether differences existed in the accuracy of the methods over a wide range of sap flux densities ranging from 5 to 80 $cm^3\,cm^{-2}\,h^{-1}$. Commercially available sensors of each type were therefore used and tested simultaneously under controlled laboratory and uncontrolled field conditions. The laboratory tests were conducted using cut stem segments of American beech (*Fagus grandifolia* Ehrh.). The field comparison of the methods was conducted over a 5-day period by placing the sensors simultaneously in a live American beech tree. Furthermore, a comprehensive error analysis was performed to determine the sources of error associated with the calculation of sap flux density with the three methods.

2. Materials and methods

2.1. Plant material

Controlled experiments were conducted in the laboratory of the Warnell School of Forestry and Natural Resources (WSFNR) of the University of Georgia near Athens, Georgia, using 10 cut stem segments of American beech (*Fagus grandifolia* Ehrh.), a diffuse-porous hardwood. Two sample trees were harvested from Whitehall forest, the experimental forest of the University of Georgia, with a 7-day time interval. The trees were 70 and 66 years old and had a stem diameter at breast height of 15 and 21 cm, respectively. Stem segments of ~1 m were brought to the laboratory in black plastic bags to minimize stem dehydration. In the laboratory, stem segments of ~25 cm were cut and prepared just before the beginning of each experiment. The three methods for measuring sap flux density (HPV, TD and HFD) were tested simultaneously and compared with measurements obtained gravimetrically.

2.2. Heat pulse method

Of the heat pulse techniques, the compensation heat pulse velocity (HPV) method has been most widely used (Edwards et al., 1996). The commercially available HPV sensor (model SF300, Greenspan Technology Pty Ltd., Warwick, Australia) used in the present study consists of a heater and two temperature-sensing probes, each containing a thermistor located 5 mm from the tip of the probe. The heater and probes were made of 1.8-mm diameter stainless steel tubing. The sensor is inserted radially into the sapwood in three vertically aligned holes. The heater is inserted into the central hole and the temperature-sensing probes are inserted in the upstream and downstream holes, 0.5 and 1.0 cm from the heater, respectively (Fig. 1). Following the release of a pulse of heat of 2 s duration into the sap stream, the temperature becomes higher at the closer upstream probe than at the downstream probe because of conduction, but heat carried by moving sap quickly warms the downstream probe so that the temperature of the two probes is again equal after a certain time (t_0). This is the time required for the heat pulse peak to move convectively with the moving sap from the heater to the mid-point between the two temperature-sensing probes (i.e. to a point 0.25 cm downstream from the heater). The time taken for the heat pulse to move this distance is used to calculate the heat pulse velocity (u, cm h^{-1}) (Swanson and Whitfield, 1981):

$$u = \frac{x_d - x_u}{2t_0} 3600 \tag{1}$$

where t_0 is the time (s) to thermal equilibration of the downstream and upstream temperature-sensing probes after release of the heat pulse, and x_d and x_u are the distances (cm) between the heater and the downstream and upstream temperature-sensing probes, respectively. Using a numerical analysis of the dissipation of a heat pulse in wood, Swanson and Whitfield (1981) showed that the measured values of u must be corrected for the influence on heat transfer of the probe construction material and for the sapwood wounding caused during the drilling procedure. The wound correction coefficients proposed by Swanson and Whitfield (1981) were used to derive corrected heat pulse velocities (u', cm h^{-1}):

$$u' = a + bu + cu^2 \tag{2}$$

where a, b and c are the corrections coefficients corresponding to the wound size (x = 0.2 cm in this study):

$$a = -11.744x^2 + 14.596x - 1.6424 \tag{3}$$

$$b = 7.2088x^2 - 6.4412x + 2.2024 \tag{4}$$

$$c = 2.3935x^2 - 0.3194x + 0.0259 \tag{5}$$

These corrected heat pulse velocities were then converted to sap flux density (SFD_{HPV}, cm^3 cm^{-2} h^{-1}) using the following equation (Marshall, 1958):

$$SFD_{HPV} = \frac{\rho_{sm} c_{sm}}{\rho_s c_s} u' = \frac{\rho_b}{\rho_s} \left(m_c + \frac{c_{dw}}{c_s} \right) u' \tag{6}$$

where ρ_{sm} is the density (g cm^{-3}) of sap plus woody matrix (including gas), c_{sm} is the specific heat capacity (J g^{-1} K^{-1}) of sap plus woody matrix (including gas), ρ_s is the density of sap, assumed equal to water (=1.0 g cm^{-3}), c_s is the specific heat capacity of sap, assumed equal to water (=4.186 J g^{-1} K^{-1}), ρ_b is the dry wood density (g cm^{-3}), m_c is the moisture content of sapwood, c_{dw} is the specific heat capacity (J g^{-1} K^{-1}) of oven-dry wood and c_{dw}/c_s is the normalized specific heat capacity of dry wood, often assumed constant at 0.33 (=1.380/4.186) (Dunlap, 1912; Edwards and Warwick, 1984). However, as the normalized specific heat of dry wood varies with temperature, a more accurate calculation was used in this study: 0.266 + 0.00116T, where T is temperature (°C) (Swanson and Whitfield, 1981). Dry wood density was calculated as:

$$\rho_b = \frac{w_d}{v_f} \tag{7}$$

where w_d is the oven-dry weight (g) and v_f is the volume of a freshly excised section of wood (cm^3). This volume was determined by immersing the fresh wood sample in water and applying Archimedes' principle. The moisture content was calculated as:

$$m_c = \frac{w_f - w_d}{w_d} \tag{8}$$

where w_f is the fresh weight (g). In the laboratory tests, freshly excised sections of stem sapwood were used for this purpose, while in the field core samples were taken using an increment borer. Averaged values for dry wood density and moisture content for both sample trees were 0.627 ± 0.056 g cm^{-3} and 0.892 ± 0.115, respectively. More details about the heat pulse method are given by Marshall (1958), Swanson and Whitfield (1981) and Smith and Allen (1996).

2.3. Thermal dissipation method

An empirical method using heat dissipation for measuring sap flux density in trees (stem diameter >40 mm) was developed by Granier (1985, 1987). The commercially available thermal dissipation probe (model TDP30, Dynamax Inc., Houston, TX, USA) consists of two 30-mm long stainless steel needles of 1.2 mm diameter which are inserted radially into the sapwood of the stem, with one needle placed approximately 40 mm above the other (Fig. 1). The upper needle contains a line heat source and a copper–constantan thermocouple junction which is referenced to another junction in the lower needle, sensing sapwood temperature. Both junctions are located 15 mm from the tip of the needle. The upper needle is supplied with a constant electric voltage (3 V for TDP30) and the difference in temperature between the two needles (ΔT) is monitored. This temperature difference is dependent on the sap flux density: heat is dissipated more rapidly when sap flux density increases and ΔT decreases as a result of the "cooling" of the heat source. From measurements on two conifers (*Pseudotsuga menziesii* (Mirb.) Franco and *Pinus nigra* Arnold) and one ring-porous hardwood species (*Quercus pedunculata* Ehrh.), Granier (1985) found experimentally that sap flux density (SFD_{TD}, cm^3 cm^{-2} h^{-1}) is related to ΔT by:

$$SFD_{TD} = 0.0119K^{1.231} 3600 \tag{9}$$

with 0.0119 and 1.231 empirically determined coefficients and the dimensionless flow index K defined as:

$$K = \frac{\Delta T_0 - \Delta T}{\Delta T} \tag{10}$$

where ΔT_0 is the value of ΔT obtained under zero flow conditions (=maximum temperature difference between the two needles) and ΔT is the measured temperature difference at a given sap flux density. An important potential limitation of this technique is that the empirical calibration has little physical basis (Smith and Allen, 1996; Clearwater et al., 1999).

2.4. Heat field deformation method

With the heat field deformation (HFD) method (Nadezhdina et al., 1998), sap flux density is derived from the sap-deformed heat field around a continuous heater (Fig. 1). Each HFD sensor consists of a heater and three needles, all 1.6-mm in diameter. Each needle contains six thermocouple junctions, spaced 6 mm apart, with the first junction located 3 mm below the cambium. The total length of each needle is 54 mm. The heater is 20 mm longer to avoid that the deepest junctions are being influenced by non-heated sap. The first needle is installed 1.5 cm above the heater (axial direction), the second needle 0.5 cm next to the heater (tangential direction) and the third needle 1.5 cm below the heater (axial direction). The first needle contains the upper junctions of the axial thermocouples, the second needle the upper junctions of the tangential thermocouples and the third needle contains the lower (reference) junctions, which are the same for the axial and tangential thermocouples. Changes in the heat field caused by moving sap are characterized by the ratio of the axial and tangential temperature differences around the heater. Calculation of sap flux density at each thermocouple junction position (SFD_{HFD}) ($cm^3\,cm^{-2}\,h^{-1}$) is based on this ratio, on the geometry of the measuring points, on the thermal diffusivity of the wood and on the sapwood depth (Nadezhdina et al., 1998, 2006):

$$SFD_{HFD} = 3600D\frac{K + dT_{sym} - dT_{asym}}{dT_{asym}} \times \frac{Z_{ax}}{Z_{tg}L_{sw}} \tag{11}$$

where D is the thermal diffusivity of fresh wood (=0.0025 $cm^2\,s^{-1}$, according to Marshall, 1958), K is the absolute value of $dT_{sym} - dT_{asym}$ under conditions of zero sap flow (°C), dT_{sym} is the temperature difference between the axial thermocouple junctions (°C), dT_{asym} is the temperature difference between the tangential thermocouple junctions (°C), Z_{ax} is the distance between the upper junction of the axial thermocouple and the heater (=1.5 cm), Z_{tg} is the distance between the upper junction of the tangential thermocouple and the heater (=0.5 cm) and L_{sw} is the sapwood depth (cm). In the laboratory tests, K was calculated as the absolute value of $dT_{sym} - dT_{asym}$ under zero flow conditions, while in the field experiment K was determined empirically from the relationship between $dT_{sym} - dT_{asym}$ and dT_{sym}/dT_{asym} (Nadezhdina et al., 2006). Depth of the sapwood was measured at the end of each experiment using green food colour to highlight the water conducting tissue of the cut stem segments. Mean sapwood depth was 4.02 ± 0.14 and 7.44 ± 0.51 cm for the sample trees with stem diameter at breast height of 15 and 21 cm, respectively.

2.5. Mariotte-based verification system

For testing the accuracy of the three sap flow methods a validation system was built using cut stem segments in which the three sensors were implanted simultaneously. Flow rates of water were held constant by maintaining a constant head of water pressure on the cut stem segments using the Mariotte's bottle principle (McCarthy, 1934) (Fig. 2). A closed water-filled 5-L Erlenmeyer flask was equipped with two glass tubes located at the same depth in the flask: one tube functioned as an air inlet, while the other, connected to a third glass tube via flexible tubing, functioned as a siphon. By adjusting the height of the flask (and thus the bottom of the air inlet), the water-filled siphon delivered the flow of water required to maintain a constant head (h = distance between the bottom of the air inlet and the surface of the cut stem segment) on the cut stem segment, regardless of the changing water level within the flask. Water passing through the cut stem segment was measured every 2–3 min using an electronic balance (model L2200S, Sartorius AG, Goettingen, Germany). Simultaneous sap flux density estimates obtained with the three sensors were compared to the actual sap flux densities. These were obtained from the rate of change in the mass of water collected and normalized for the conducting sapwood area. Conducting sap wood area was measured on the coloured stem segments at the end of each experiment. The verification system was used to test sap flux densities ranging from 5 to 80 $cm^3\,cm^{-2}\,h^{-1}$, which is within the range of values reported in the literature (Granier, 1985). To this end, constant heads of water of 2, 5, 10, 15 and 25 cm were maintained on every cut stem segment for at least a half hour.

2.6. Sap flow units

Despite the attempt of Edwards et al. (1996) to coordinate a unified nomenclature for sap flow measurements, a mixture of units is still in use in literature to express sap velocities, fluxes and flows. The greatest misconception is that sap flux densities can be expressed as sap velocities. The reasoning behind this erroneous use is that the cubic centimetres (cm^3) of sap flowing across each cm^2 of sapwood perpendicular to the direction of flow per unit time would be identical to the distance (cm) that the sap has travelled per unit of time. In physics, this is only valid when the area across which the sap is moving consists of sap (volume (cm^3) = distance (cm) × area (cm^2)); an assumption that does not hold for the conducting sapwood tissue in stems. Based on this reflection, HPV, TD and HFD values (as defined in Eqs. (6), (9) and (11), respectively) must be expressed in sap flux density units (i.e. $cm^3\,cm^{-2}\,h^{-1}$) instead of, the often wrongly used, velocity units (i.e. $cm\,h^{-1}$) (see for instance some original methodological papers: Granier, 1987).

2.7. Measurement protocol: from sample preparation to sensor installation

All laboratory tests were performed at a constant room temperature of 25.4 ± 0.5 °C. After sawing a 25-cm long stem segment from a fresh American beech log, both cut surfaces were wetted and trimmed using a razor blade to re-open possibly closed vessels. The bark at the top of the stem segment (a 2-cm strip) was removed to ensure that water only passed through the stem xylem. Next, a 30-cm high cylinder made of 0.18 mm mylar film (Ridout Plastics, San Diego, CA, USA) was fixed directly to the xylem using silicone and double-sticking adhesive tape. Silicone was further used to make the connection between stem and plastic cylinder water impermeable. After a drying phase of ∼18 h, during which stem dehydration was prevented by moistening top and bottom, the cut stem segment was prepared for sensor installation. As with all sap-flow techniques, it was essential that the heater and sensors probes/needles were correctly positioned. Accurate vertical spacing and parallel drilling was achieved by using the appropriate drilling template supplied with the sensors. To avoid any misalignment of the heater and/or sensor probes/needles, the drilling of the holes was done carefully using a drill press (model SM300, Delta Machinery, Jackson, TN, USA). The required set of holes for each sensor were drilled at an angle of 120° from each other and were arranged randomly in the vertical direction. TD and HPV sensors were installed to measure sap flux densities at 15 mm below the cambium, while HFD sensors measured sap flux densities at 3, 9, 15, 21, 27 and 33 mm below the cambium. The prepared stem segment was subsequently suspended in the Mariotte-based verification system (Fig. 2) and the sensors were installed. Before installation in the stem segment, heater and probes/needles were coated with silicone grease. The sensors were thermally insulated with open-cell foam, which was a prerequisite for accurate measurements, despite the constant air temperature inside the laboratory. The HPV system was supplied with a logging and control unit which controlled the pulsing of the heater and recorded the measurements at intervals of 3 min. Preliminary tests had shown that this logging frequency yielded equal results compared to 10-min intervals or longer. Individual thermocouples of the TD and the HFD sensors were connected to a 64-channel multiplexer (Model AM416, Campbell Scientific Inc., Logan, UT, USA) which in turn was connected to a data logger (Model CR23X, Campbell Scientific Inc., Logan, UT, USA). Measurements were made every 10 s.

Because the TD method requires a period of zero flow conditions (Eq. (10)), all sensors installed were logged during ∼2 h without passing any water through the stem segment. Next, the stem segment was flushed with distilled water for 15–30 min. When the balance readings stabilised, the water was removed and constant flow rates were maintained using the Mariotte-based verification system. Prior to the start of the validation experiments, the potential interference of heat from the simultaneously installed sensors

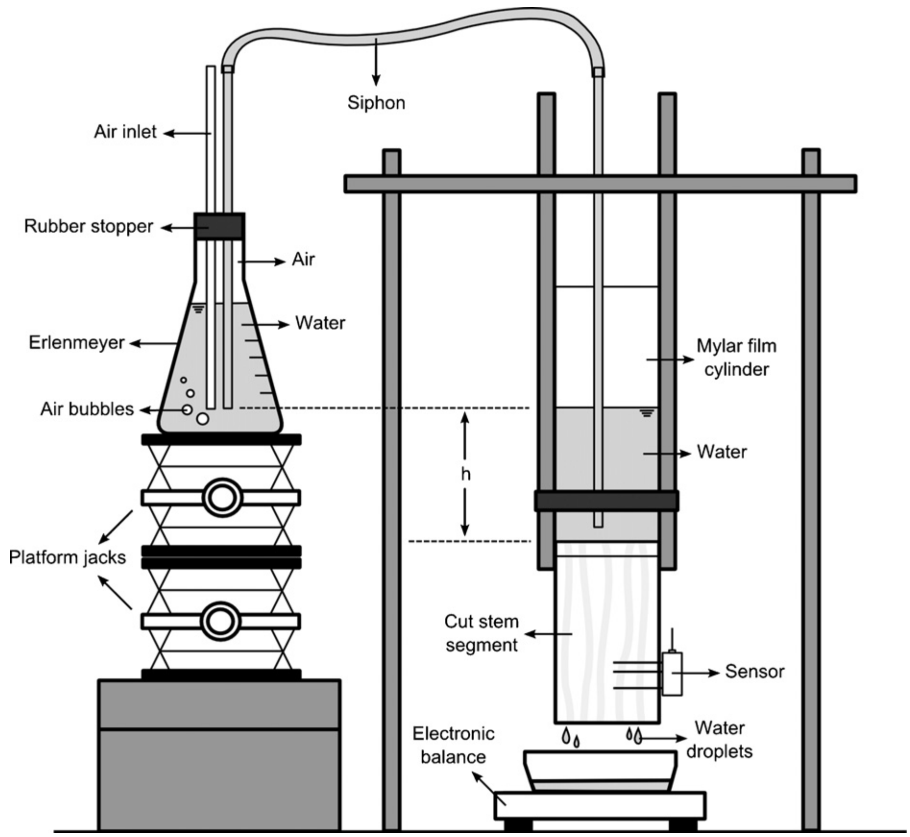

Fig. 2. Schematic diagram of the Mariotte-based verification system used for testing the accuracy of the three sap flow methods.

was investigated in an experiment with a small cut stem segment using a constant head of water pressure. No thermal interference could be observed when the heater of each of the installed sensors was alternatively switched on and off (data not shown). This result justified the simultaneous use of different sensors in further experiments.

In total, 10 cut stem segments were used: nine for testing the accuracy of the sensors and one for testing the circumferential variability in sap flux density in a cut stem segment. To perform the later test, the sensors were rotated clockwise every hour at an angle of 120° using a constant head of water pressure of 5 cm on the cut stem segment.

2.8. Field experiment

The field comparison of the three methods was conducted over a 5-day period (21–25 July 2008) by placing the sensors simultaneously in a live American beech tree in Whitehall forest. Stem diameter at sensor installation height was 19.9 cm. All sensors were placed in a horizontal plane ~90 cm above soil surface. The sensors were arranged around the stem circumference, spaced 90° from each other: two HPV sensors were installed on opposing sides of the stem, while the TD and the HFD sensor were installed perpendicular to this direction, also on opposing sides of the stem. The TD and HPV sensors measured sap flux densities at a depth of 15 mm, while the HFD sensor measured sap flux densities at 3, 9, 15, 21, 27 and 33 mm depth. HPV was recorded at intervals of 10 min with the supplied logging unit, while TD and HFD were logged at 1-min intervals using a multiplexer (Model AM416, Campbell Scientific Inc., Logan, UT, USA) connected to a battery-powered data logger (Model CR23X, Campbell Scientific Inc., Logan, UT, USA).

2.9. Radial profile correction for single point sensors

The effect of radial variability in sap flux density was examined during the laboratory tests. The single point sap flux density measurements obtained with TD and HPV were therefore scaled to account for the radial sap flux profile measured with the HFD method. To this end, measured HFD sap flux density at each depth was divided by that measured at 15 mm depth to obtain a ratio. Next, sap flux densities at the non-measured depths were estimated as the product of the ratio at that depth and the actual TD or HPV value measured at 15 mm depth.

2.10. Sap flux density error analysis

Errors in sap flux density calculation resulting from an inaccurate setting of parameters in the equations were evaluated using a sensitivity analysis. The sensitivity analysis was performed with data from the third replicate of the lab experiment, but yielded similar results for the other experiments. For each sap flow method, two sap flux density values were selected and used as reference value: the low value corresponding with the first step and the high value corresponding with the last step (Fig. 3). Both the low and the high reference value represent the respective measured sensor value. Relative sap flux density errors were expressed as percentage overestimation or underestimation of these selected reference values. For each method, all relevant parameters that might be prone to error were selected: $x_d - x_u$, x, w_f, w_d, v_f and c_{dw}/c_s for HPV (Eqs. (1)–(8)); a, b and ΔT_0 for TD (Eqs. (9) and (10)) and D, K, Z_{ax}/Z_{tg}, L_{sw} for HFD (Eq. (11)). Calculations were performed for increasing errors of these parameters (±5, 10, 20 and 40%), maintaining all the other parameters at their original values.

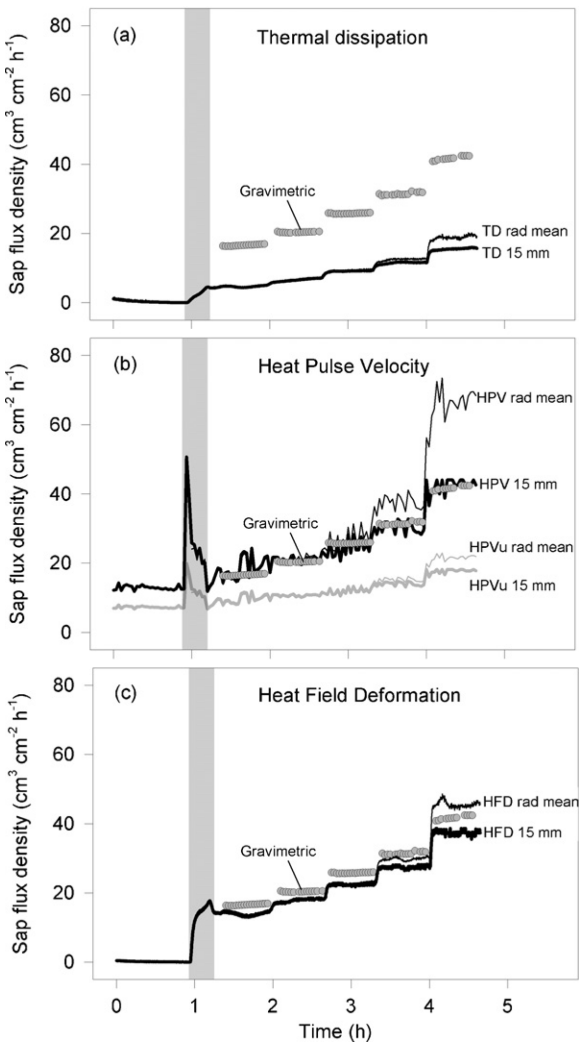

Fig. 3. A typical response of simultaneously measured TD (a), HPV (b) and HFD (c) sap flux densities to stepwise changes in flow rate through a cut stem segment in American beech. For HPV, sap flux densities are calculated with (HPV) and without (HPVu) taking the wound correction into account. Sap flux densities measured at 15 mm depth and scaled for the radial profile (rad mean) are compared with the gravimetrically obtained ones. The grey area represents the flushing period with distilled water.

3. Results

3.1. Response of sap flux density estimates to stepwise changes in flow rate

A typical response of simultaneously measured TD, HPV and HFD sap flux densities to stepwise changes in flow rate through a cut stem segment is shown in Fig. 3. Sap flux density measured at 15 mm depth increased with increasing flow rates. The time constant of the transient response of the sensors' output when flow rate in the cut stem segment suddenly changed was established through non-linear regression with an exponential curve (Chu et al., 2009). The time constants (time to reach 63% of the maximum value) were 0.1, 1.6 and 0.6 min for HPV, TD and HFD, respectively, indicating that the sensors' response from one flow rate to another is rather fast. Despite the fast observed response, the use of heat pulses limited the HPV measurement interval to 3 min or higher due to the necessity to regain equilibrium in the sapwood before a next heat pulse can be released. When comparing the noise level on the sensors' output when flow rates were kept constant, larger fluctuations were observed for HPV compared to TD or HFD.

Sap flux densities measured by HPV and HFD at 15 mm depth corresponded closely with that measured by the electronic balance. TD clearly underestimated the actual flow rate. The close agreement between HPV and the balance measurements was only obtained when wound correction was included in the calculation (Fig. 3b). HPV was, however, unable to resolve zero sap flux measurements. For instance, in the third replicate of the experiment at zero flow, sap flux densities of $12.9 \pm 0.6\,\mathrm{cm^3\,cm^{-2}\,h^{-1}}$ ($u = 8.2 \pm 0.3\,\mathrm{cm\,h^{-1}}$) were derived instead (Fig. 3b).

3.2. Radial variability of HFD sap flux density estimates in cut stem segments

The response of sap flux densities measured by HFD at six depths in two cut stem segments to stepwise changes in flow rate is shown in Fig. 4. Despite the use of a constant water head pressure above the cut stem segments, a strong radial variability in sap flux density was observed. This radial variability was greatly dependent on the selected stem segment, with the measurements at individual positions being lower and/or higher than the ones obtained with the balance. In order to better visualise the radial sap flux density profile, measured values were plotted in function of the sapwood depth (Fig. 5). The profiles became more pronounced with increasing imposed sap flux densities. While the overall shape of the individual profiles remained the same within one segment, they were different between stem segments.

The effect of including the radial profile in sap flux density calculations is illustrated in Fig. 3. Single point measurements at 15 mm depth are compared to radial mean sap flux densities, taking into account the radial profile (as described in Section 2.9) and averaging over the six depths. Only at higher sap flux densities a clear difference could be observed. The observation that HPV measurements at 15 mm depth at high sap flux densities match the gravimetric ones more closely than HPV corrected for the radial profile was not generally valid. This was confirmed when evaluating the overall result from the HPV probe (Fig. 6c) which shows that only experiments 3 (of which the time series are shown in Fig. 3b) and 4 are above the 1:1 line and, hence, overestimate the gravimetric measurements, particularly at higher sap flux densities.

3.3. Validation and error analysis of sap flux density estimates in cut stem segments

The relationship between balance measurements and sensor sap flux density estimates for all experiments is shown in Fig. 6. Radial mean sap flux densities were used for the assessment of the sensors' accuracy: for each imposed flow rate, the averaged radial mean sap flux density was calculated. Standard deviations confirmed the larger noise level in measurements made with HPV compared to TD or HFD.

Strong linear relationships were observed within each individual experiment ($R^2 > 0.98$). Despite the use of the same stepwise increasing heads of water pressure in each experiment, different sap flux densities for different stem segments were measured with the balance, ranging from 5 to 80 $\mathrm{cm^3\,cm^{-2}\,h^{-1}}$. The highest sap flux densities were only achieved in experiments with stem segments of larger diameters, while the lower part of this range was covered by experiments with smaller diameter stem segments. Because the slope of the individual relationships differed, a large overall variability was observed.

There were significant differences in the estimates of sap flux density from each of the three methods (Fig. 6). Overall, all sensors underestimated the actual sap flux density and this error became more pronounced with increasing sap flux density. While there were systematic errors in the TD measurements, the errors differed for different stem segments when considering the HFD or

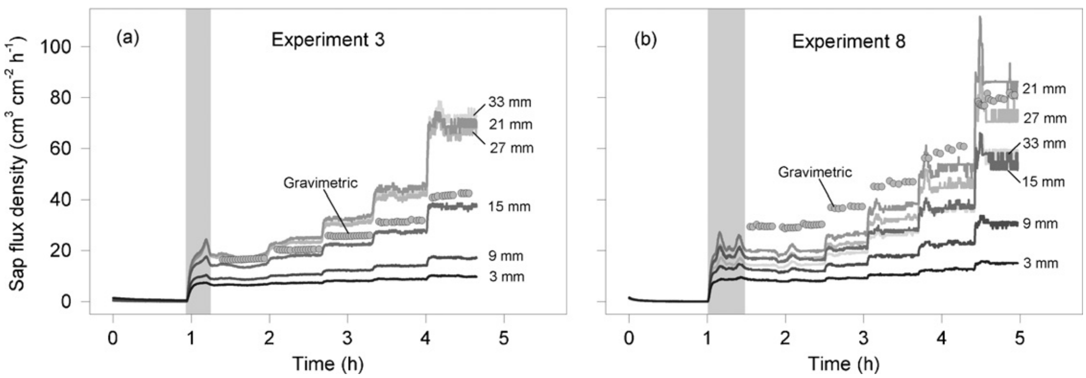

Fig. 4. The response of HFD sap flux densities measured at six depths in two cut stem segments in American beech (a: experiment 3 and b: experiment 8) to stepwise changes in flow rate. Each depth is indicated by a label. The grey area represents the flushing period with distilled water.

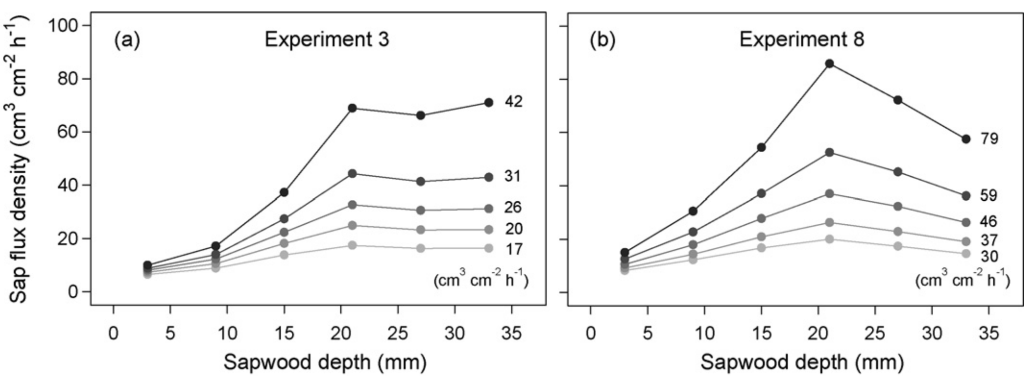

Fig. 5. Radial sap flux density profiles measured in two cut stem segments of American beech (a: experiment 3 and b: experiment 8). The effect of increasing imposed sap flux densities on the radial profile is shown. Each imposed sap flux density is indicated by a label and expressed in $cm^3\ cm^{-2}\ h^{-1}$.

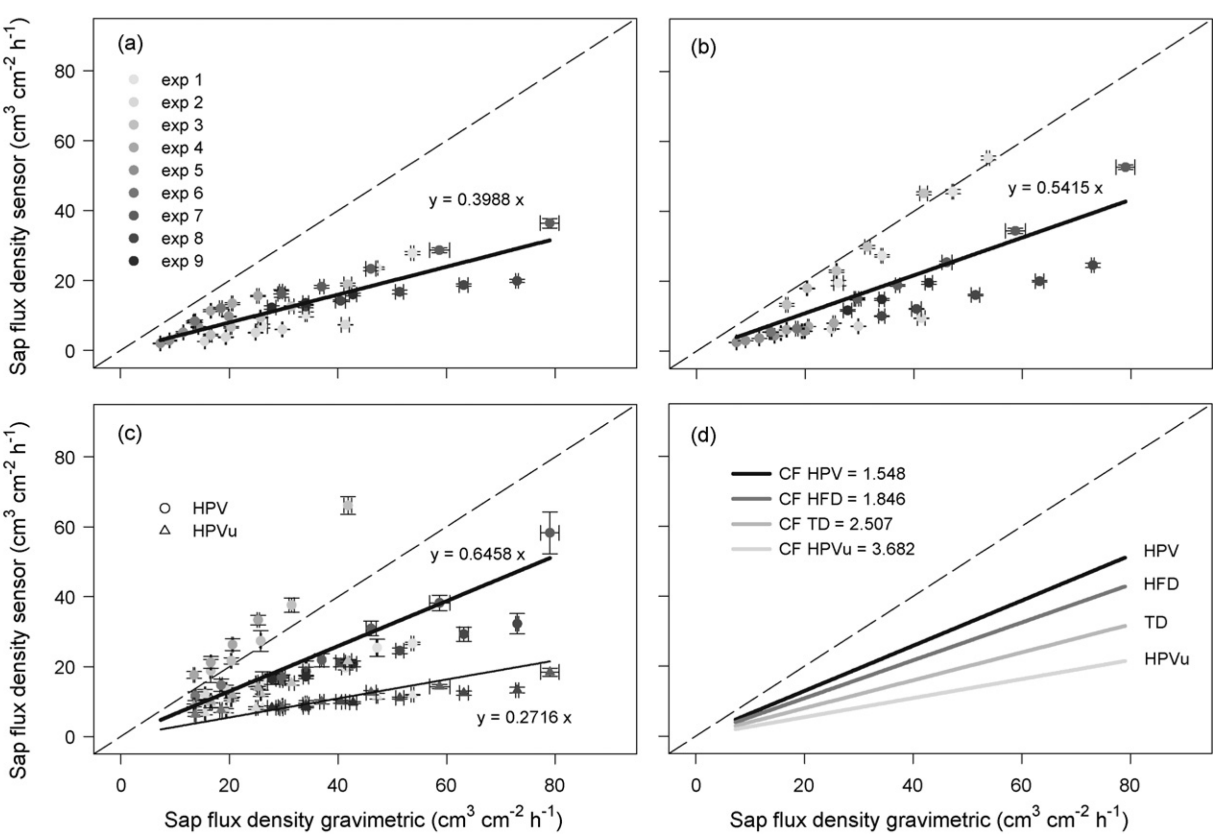

Fig. 6. Comparison of sap flux densities measured with the TD (a), the HFD (b) and the HPV (c) method and actual sap flux densities measured with the balance (gravimetric). Nine cut stem segments of American beech were used and in each experiment at least four different constant heads of water pressure were applied. Single point measurements were corrected for the radial sap flux profile and averaged over the depth. A correction factor (CF) for each method was calculated as the inverse of the slopes of each regression line (d).

HPV results. For instance, the TD slope for experiment 3 was identical to that of its overall relationship (0.3998, $R^2 = 0.9021$), while an overestimation was found for HPV (1.3201, $R^2 = 0.8532$) and quasi unity for HFD (0.9774, $R^2 = 0.941$). Overall, the most accurate measurements were made with HPV, but only after applying a wound correction. The least accurate measurements proved to be TD, which is presently the most commonly used method. There was an average error between actual and estimated sap flow density of 35% using HPV, 46% using HFD and 60% using TD. The reciprocal of the calculated slopes yielded correction factors of 1.548, 1.846 and 2.507, respectively (Fig. 6d).

3.4. Circumferential variability of sap flux density estimates in cut stem segments

Part of the overall variability observed in Fig. 6 may arise from circumferential heterogeneity in the wood tissue. To validate this assumption, a sensor rotation experiment was carried out (Fig. 7). Circumferential variability was detectable in the cut stem segment despite the use of the constant water pressure head. Indeed, a sim-

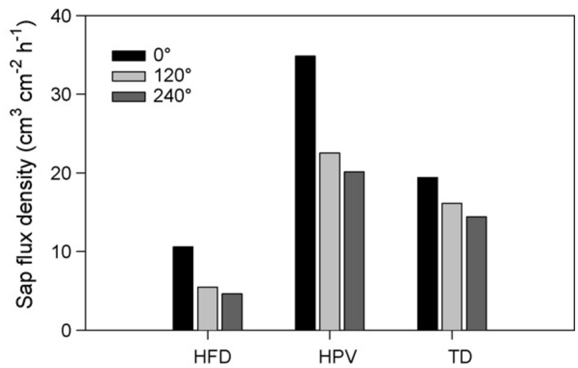

Fig. 7. Circumferential heterogeneity in a cut stem segment of American beech during a sensor rotation experiment with a constant water pressure head of 5 cm on the cut stem segment.

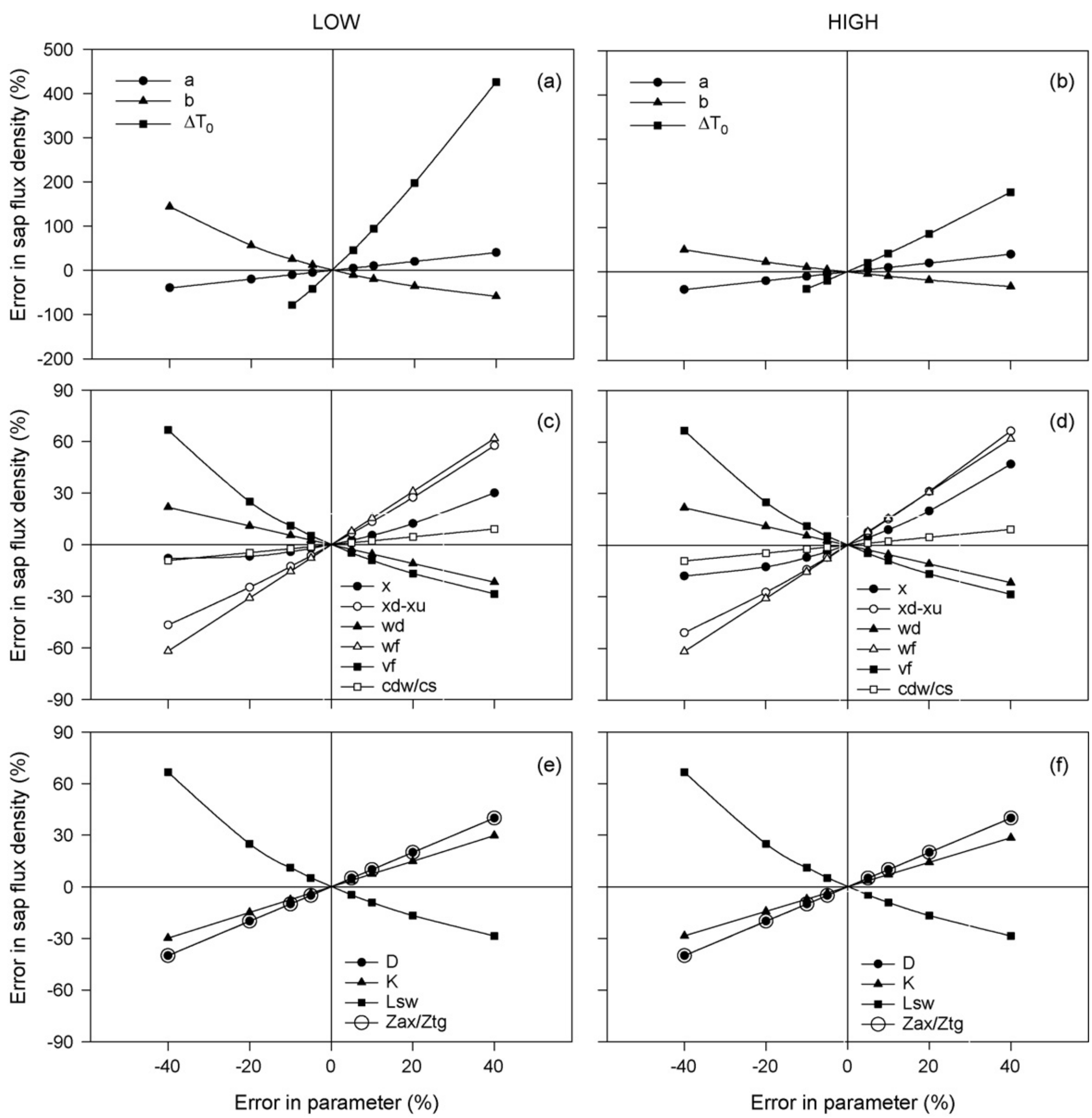

Fig. 8. Sap flux density error analysis illustrating the resultant error in sap flux density from TD (a and b), HPV (c and d) and HFD (e and f) due to errors in selected parameters in the equations while maintaining all other parameters at their original value. The error analysis was based on the third lab experiment (Fig. 3) and includes the lowest and the highest imposed sap flux density.

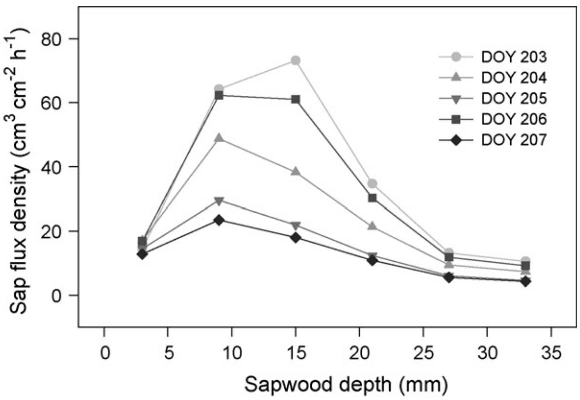

Fig. 9. Radial sap flux density profiles measured in a live American beech tree in the field at different consecutive days (DOY: day of year) with the HFD sensor.

ilar decrease in sap flux density estimates for each method was detected when the sensor was installed at the 0°, 120° or 240° position, respectively, although the absolute values differed between the methods used.

3.5. Sap flux density error analysis

As expected, parameter errors resulted in errors of the calculated sap flux densities (Fig. 8). Between the two considered sap flux density situations (low and high) no real differences could be observed, except for TD which had larger errors for the low flux density case. For HFD all errors remained identical for both low and high sap flux density, with the exception of the slightly different errors related to the parameter K (Fig. 8e and f).

Based on the sensitivity analysis an importance ranking of the parameters was established to offer additional insights into potential causes of errors: $\Delta T_0 > b > a$ for TD; $w_f > x_d - x_u > v_f > w_d > x > c_{dw}/c_s$ for HPV and $D = Z_{ax}/Z_{tg} > L_{sw} > K$ for HFD. The equal contribution of D and Z_{ax}/Z_{tg} for HFD is attributed to the multiplication effect that both parameters have in Eq. (11). The ranking was established for small parameter errors (±5%; most likely to occur in practice) and resulted in small errors for HPV and HFD (<8%) but in large errors for TD (41%). For large parameter errors (40%) the latter even increased to 400%, while those for HPV and HFD remained limited to ~70%. For small errors, all parameters reacted nearly linear and the non-linearity of some of the parameters only became pronounced at higher error values causing certain parameters to switch position in the importance ranking (Fig. 8).

In addition, while the sap flux density and parameter errors increased in the same direction in some cases, an opposite response was detected for other cases. This is, for example, illustrated for the empirical parameters a and b for TD. A +5% error in both parameters would cause the resulting error in sap flux density to be masked.

3.6. Comparison of sap flux density estimates in a beech tree in the field

In order to verify the lab findings, a comparison of concurrent sap flux density measurements acquired by the three methods in an actively transpiring beech tree in the field was made. To this end, the radial profile existing in the live sampled tree was taken into account (Fig. 9). Sap flux density was always greatest in the outer 15 mm of sapwood and lowest in the inner 20–35 mm sapwood, but the specific midday pattern of the radial profile changed from day to day. This change in radial profile was related to the magnitude of the stem sap flux density: the radial profile became more pronounced with higher sap flux densities (Fig. 9). This finding is in agreement with the earlier results obtained with the cut stem segments (Fig. 5). The midday radial profiles assessed during maximum flow rates (1–3 pm) were used to scale the HPV and TD point measurements spatially to the whole sap wood area. This scaling strategy was adopted because HFD measurements at 15 mm depth in the sampled tree displayed a slower increase of sap flux density early in the morning and a faster decrease in the late afternoon compared to the other two sap flow methods. This specific difference in the pattern's dynamics necessitated the use of midday mean radial profiles instead of the continuously measured HFD radial profiles.

The scaled field data provided comparable results as the ones obtained in the lab: while the diurnal pattern of sap flux density for HPV and HFD was similar (with values of either HPV or HFD greatest), the diurnal pattern for TD was typically lowest (Fig. 10a).

The strong agreement in daily HPV pattern measured at the opposite sides of the tree stem indicated that circumferential variability in the sampled beech tree was rather low. The inability of HPV to resolve zero sap flux density measurements was confirmed in the field test by the higher and noisier signals compared to HFD or TD.

The similar conclusions regarding sensor performance that can be drawn from the lab and the field study suggest that the correction factors obtained on cut stem segments might also be applicable in the field. Therefore, the respective factors were used to correct the sap flux densities (Fig. 10b) resulting in almost identical actual sap flux densities for each method. Noteworthy is that these actual sap flux densities were almost double of the originally calculated values.

4. Discussion

4.1. Measurement accuracy of sap flux density estimates

This is the first report of an accuracy test of and comparison between the HPV, HFD and TD method applied synchronously. The results demonstrated that significant differences existed in the estimates of sap flux density from each of the three methods. The actual sap flux density was seriously underestimated by all three methods, with the error increasing with sap flux density (Fig. 6). Higher potential errors with higher sap flux densities were also reported for TD by Clearwater et al. (1999). Overall the most accurate method was HPV, but only after applying the published wound correction of Swanson and Whitfield (1981). The remaining deviation for HPV might be caused by either inadequacy of the published wound correction for American beech or by thermal heterogeneity of the sapwood. Indeed, if the distribution of the vessels in the sapwood is markedly non-uniform, or if the distances between the vessels are too large (>0.4 mm according to Swanson (1983)) for the time required for thermal equilibration between sap and woody matrix to be considered negligible, HPV calculations are likely to be in error (Marshall, 1958; Swanson and Whitfield, 1981; Green and Clothier, 1988; Swanson, 1994; Smith and Allen, 1996). Also Smith and Allen (1996) concluded that thermal heterogeneity due to vessel spacing exceeding the 0.4 mm threshold caused an underestimation of the actual sap flux density and, hence, required a correction factor of 1.62 for *Azadirachta indica* A. Juss.

Although the issue of thermal heterogeneity was reported in the context of the HPV method, its effects might also influence the readings of the HFD and TD sensors and partially explain the underestimation of the measured sap flux densities. In addition, the finding that TD was the least accurate sensor is probably also related to the fact that the method is not based on physical principles of heat transfer.

The substantial improvement in the accuracy of the HPV method after using a wound correction suggest the HFD and TD methods might require similar methodological improvements. A simple

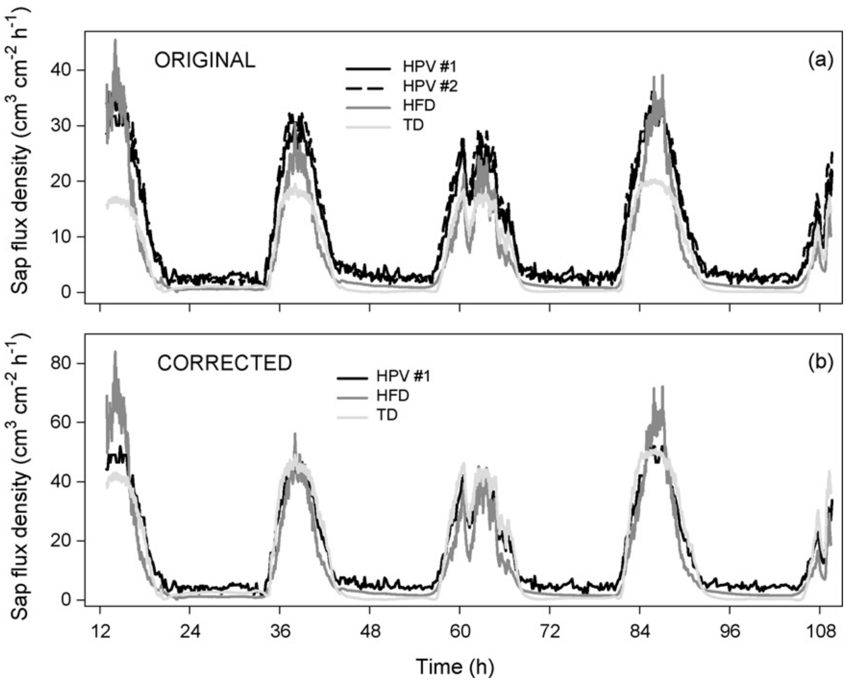

Fig. 10. A comparison of concurrent sap flux density measurements acquired by the HPV, TD and HFD method in an actively transpiring American beech tree in the field: (a) originally calculated sap flux densities taking into account the radial profile of the sampled tree (Fig. 9); (b) corrected sap flux densities using the correction factors determined in the validation experiment (Fig. 6d).

extrapolation of the published wound correction method (Swanson and Whitfield, 1981) is, however, not possible, because the proposed correction factors should be applied to the heat pulse velocity and not to the sap flux density. While Swanson and Whitfield (1981) found that a quadratic correction function was most suitable, our results do not support this. A linear transformation was found to be more appropriate. The corresponding correction factors for our beech tree were 1.55, 1.85 and 2.5 for HPV, HFD and TD, respectively (Fig. 6d). Moreover, this simplification towards a linear approximation was also adopted by Burgess et al. (2001) for his improved heat pulse method.

Although the HPV method was the most accurate one, it had the highest noise level, especially at low flux densities. This high noise level during zero measurements is a well-known limitation of the HPV sensor, often corrected by using a cut-off value, and is caused by the dissipation of the heat pulse via conduction before it can reach the measurement point (Becker, 1998; Burgess et al., 2001). Overestimation of the near zero velocities are further exacerbated by the used wound correction functions (Burgess et al., 2001). In contrast, noise levels were negligible for TD and HFD. One drawback of TD is the assumption of zero flux conditions necessary to calculate ΔT_0. Zero flow conditions can be guaranteed in lab experiments, but are uncertain in any field trial. In addition, drift in ΔT_0 can occur between different nights due to variation in wood water content which influences thermal dissipation (Do and Rocheteau, 2002). HFD deals with this issue by estimating a value for K which corresponds to zero flow by relating $(dT_{sym} - dT_{asym})$ to dT_{sym}/dT_{asym}. The use of this regression line allows extrapolation to zero flow (i.e. $dT_{sym}/dT_{asym} = 0$) if necessary.

4.2. Sap flux density error analysis

The parameter importance ranking offered further insights into potential causes of errors and revealed that parameters associated with sensor positioning ($x_d - x_u$ for HPV and Z_{ax}/Z_{tg} for HFD) are highly sensitive and therefore drilling should be performed with the highest possible accuracy (Fig. 8). For HFD, a correct setting of the parameter D appears to be equally important (Fig. 8). However, in practice, the standard value proposed by Marshall (1958) is used throughout the HFD literature. A major disadvantage of the HFD calculation method is its strong dependence on L_{sw}. Especially in trees with larger or difficult to define sapwood depths, L_{sw} might be a considerable source of error in HFD sap flux density estimates (Fig. 8).

The ranking also pointed out that the wound width (x) which is often considered as one of the most crucial parameters for HPV (e.g., Swanson and Whitfield, 1981; Dye et al., 1996; Smith and Allen, 1996; Bleby et al., 2004) was less sensitive than expected. A 5% error in x only caused a 4.3% error in sap flux density, while a similar error in w_f resulted in a 7.7% error. Therefore, precautions should be taken, especially in the field, to allow for a correct fresh weight determination of the sap wood sample (w_f).

For TD, the high errors associated with parameters a and especially b result from the empirical power function originally defined by Granier (1985). A recalibration of this original equation, based on the data of the lab experiment, resulted in 0.0230 for a and 0.9519 for b ($R^2 = 0.7039$) illustrating that the originally proposed values were +93.0% and −22.7% in error for American beech. This resulted in an overall 143.0% error in the sap flux density (i.e. 2.430 times the sap flux density calculated with Eq. (9)), which is nearly identical to the proposed linear correction factor for TD (i.e. 2.507) (Fig. 6d). In addition, the high error associated with ΔT_0 (Fig. 8) and the uncertainty of the assumption of zero flow conditions in living trees (Regalado and Ritter, 2007) indicates that this parameter needs to be handled with great care.

There appeared to be no single reason why the three techniques underestimated actual sap flux density, but rather multiple errors likely occurred, compounding to reduce the overall accuracy of each technique. Despite the ideal test environment in this study (i.e. constant flow rates and isothermal stem and air temperatures rather than variable flow rates and temperature as in sun/shade conditions or changing vapour pressure deficits), the errors were of a magnitude to be concerned about the accuracy of all three techniques. Errors encountered in field studies are likely to be even greater. All techniques used today, ranging from the empirical TD to the more physically based HPV and HFD, remain simplifications of reality. Recalibration for each new tree species on which these techniques are used might be necessary, at least until a physically based error correction protocol is established or new approaches for calculating sap flux density emerge.

4.3. Radial and circumferential variability in cut segments

Radial and circumferential variability in sap flux density is a well-known fact in actively transpiring trees and has been observed in many studies. This variability has been related to atmospheric variables (vapour pressure deficit and photosynthetic active radiation), rhizospheric variables (soil water availability) and structural variables (crown architecture) (Phillips et al., 1996; Nadezhdina et al., 2002; Ford et al., 2004a,b; Fiora and Cescatti, 2006; Saveyn et al., 2008).

One would expect that in cut stem experiments using a constant pressure head of water the radial and circumferential variability would disappear. However, significant radial and circumferential variability remained present in our study. Bleby et al. (2004) argued that circumferential and radial patterns may be radically altered while cutting the stem segments. Indeed, in comparison with a non-cut tree, changes in the profiles might occur from improper stem segment preparation resulting in excessive tissue damage. However, despite the use of the constant pressure head and the absence of other driving variables a strikingly similar response to changes in water flow was observed in the cut stem segments compared to the field tree: higher flux densities resulted in more pronounced radial profiles (Figs. 5 and 9). Also circumferential variability within a stem segment remained (Fig. 7). These findings indicate that radial and circumferential variability cannot be ignored, even in cut stem experiments, and thus have important implications for future sap flow validation experiments.

4.4. Estimation of actual sap flux densities in the field

For the live sampled beech tree, the corrected sap flux densities of the different methods were almost identical (Fig. 10b). This successful extrapolation from the lab to the field gave confidence in the correction factors obtained for American beech. Although in this study, this transfer of correction factors proved valid, it should still be determined if they are also applicable for other species. Given the magnitude of the obtained correction factors, validation of sap flow methods remains an important concern when accurate estimates of the water budget of tree-dominated ecosystems are required.

Acknowledgements

The authors wish to thank the Fund for Scientific Research—Flanders (FWO) for the postdoctoral fellow grant and the travel funding granted to KS. We also wish to thank Timothy Wertin for his help with cutting stem segments, the staff of the School of Forestry and Natural Resources (UGA) for safely cutting down the trees in the UGA experimental forest and Nadja Nadezhdina and Jan Čermák for supplying the HFD sensors.

References

Ansley, R.J., Dugas, W.A., Heuer, M.L., Trevino, B.A., 1994. Stem flow and porometer measurements of transpiration from honey mesquite (*Prosopis glandulosa*). J. Exp. Bot. 45, 847–856.

Becker, P., 1998. Limitations of a compensation heat pulse velocity system at low sap flow: implications for measurements at night and in shaded trees. Tree Physiol. 18, 177–184.

Bleby, T.M., Burgess, S.S.O., Adams, M.A., 2004. A validation, comparison and error analysis of two heat-pulse methods for measuring sap flow in *Eucalyptus marginata* saplings. Funct. Plant Biol. 31, 645–658.

Burgess, S.S.O., Adams, M.A., Turner, N.C., Beverly, C.R., Ong, C.K., Khan, A.A.H., Bleby, T.M., 2001. An improved heat pulse method to measure low and reverse rates of sap flow in woody plants. Tree Physiol. 21, 589–598.

Chu, C.R., Hsieh, C.-I., Wu, S.-Y., Phillips, N.G., 2009. Transient response of sap flow to wind speed. J. Exp. Bot. 60, 249–255.

Clearwater, M.J., Meinzer, F.C., Andrade, J.L., Goldstein, G., Holbrook, N.M., 1999. Potential errors in measurement of nonuniform sap flow using heat dissipation probes. Tree Physiol. 19, 681–687.

Dixon, H.H., 1937. The Convection of Heat and Materials in the Stem of a Tree, vol. 4. Notes Botanical School, Trinity College, Dublin, pp. 269–278.

Do, F., Rocheteau, A., 2002. Influence of natural temperature gradients on measurements of xylem sap flow with thermal dissipation probes. 1. Field observations and possible remedies. Tree Physiol. 22, 641–648.

Dunlap, F., 1912. The specific heat of wood. USDA Forest Service Bulletin No. 110, 28 pp.

Dye, P.J., Soko, S., Poulter, A.G., 1996. Evaluation of the heat pulse velocity method for measuring sap flow in *Pinus patula*. J. Exp. Bot. 47, 975–981.

Edwards, W.R.N., Becker, P., Čermák, J., 1996. A unified nomenclature for sap flow measurements. Tree Physiol. 17, 65–67.

Edwards, W.R.N., Warwick, N.W.M., 1984. Transpiration from a kiwifruit vine as estimated by the heat pulse technique and the Penman–Monteith equation. New Zeal. J. Agric. Res. 27, 537–543.

Fiora, A., Cescatti, A., 2006. Diurnal and seasonal variability in radial distribution of sap flux density: implications for estimating stand transpiration. Tree Physiol. 26, 1217–1225.

Ford, C.R., Goranson, C.E., Mitchell, R.J., Rodney, E.W., Teskey, R.O., 2004a. Diurnal and seasonal variability in the radial distribution of sap flow: predicting total stem flow in *Pinus taeda* trees. Tree Physiol. 24, 951–960.

Ford, C.R., McGuire, M.A., Mitchell, R.J., Teskey, R.O., 2004b. Assessing variation in the radial profile of sap flux density in *Pinus* species and its effect on daily water use. Tree Physiol. 24, 241–249.

Ford, C.R., Mitchell, R.J., Teskey, R.O., 2008. Water table depth affects productivity, water use, and the response to nitrogen addition in a savanna system. Can. J. Forest Res. 38, 2118–2127.

Granier, A., 1985. Une nouvelle méthode pour la mesure du flux de sève brute dans le tronc des arbres. Ann. Sci. Forest. 42, 193–200.

Granier, A., 1987. Evaluation of transpiration in a Douglas-fir stand by means of sap flow measurements. Tree Physiol. 3, 309–319.

Green, S.R., Clothier, B.E., 1988. Water-use of kiwifruit vines and apple-trees by the heat-pulse technique. J. Exp. Bot. 39, 115–123.

Huber, B., 1932. Beobachtung und Messung pflanzlicher Saftströme. Ber. Deutsche Bot. Ges. 50, 89–109.

Huber, B., Schmidt, B., 1937. Eine Kompensationmethode zur thermoelektrischen Messung langsamer Saftströme. Ber. Deutsche Bot. Ges. 55, 514–529.

Ittner, E., 1968. Der Tagesgang der Geschwindigkeit des Transpirationsstromes im Stam einer 75-jaehrigen Fichte. Oecol. Plant. 3, 177–183.

Marshall, D.C., 1958. Measurement of sap flow in conifers by heat transport. Plant Physiol. 33, 385–396.

McCarthy, E.L., 1934. Mariotte's bottle. Science 80, 100.

Mitchell, P.J., Veneklaas, E., Lambers, H., Burgess, S.S.O., 2009. Partitioning of evapotranspiration in a semi-arid eucalypt woodland in south-western Australia. Agric. Forest Meteorol. 149, 25–37.

Nadezhdina, N., Čermák, J., Ceulemans, R., 2002. Radial patterns of sap flow in woody stems of dominant and understory species: scaling errors associated with positioning of sensors. Tree Physiol. 22, 907–918.

Nadezhdina, N., Čermák, J., Gašpárek, J., Nadezhdin, V., Prax, A., 2006. Vertical and horizontal water redistribution in Norway spruce (*Picea abies*) roots in the Moravian Upland. Tree Physiol. 26, 1277–1288.

Nadezhdina, N., Čermák, J., Nadezhdin, V., 1998. Heat field deformation method for sap flow measurements. In: Čermák, J., Nadezhdina, N. (Eds.), Proceedings of the 4th International Workshop on Measuring Sap Flow in Intact Plants. Publishing House of Mendel University, Czech Republic, pp. 72–92.

Phillips, N., Oren, R., Zimmermann, R., 1996. Radial patterns of xylem sap flow in non-, diffuse- and ring-porous tree species. Plant Cell Environ. 19, 983–990.

Regalado, C.M., Ritter, A., 2007. An alternative method to estimate zero flow temperature differences for Granier's thermal dissipation technique. Tree Physiol. 27, 1093–1102.

Saveyn, A., Steppe, K., Lemeur, R., 2008. Spatial variability of xylem sap flow in mature beech (*Fagus sylvatica*) and its diurnal dynamics in relation to microclimate. Botany 86, 1440–1448.

Schurr, U., 1998. Xylem sap sampling—new approaches to an old topic. Trends Plant Sci. 3, 293–298.

Smith, D.M., Allen, S.J., 1996. Measurement of sap flow in plant stems. J. Exp. Bot. 47, 1833–1844.

Swanson, R.H., 1983. Numerical and experimental analysis of implanted-probe heat pulse velocity theory. Ph.D. Thesis, University of Alberta, Edmonton, Canada, 298 pp.

Swanson, R.H., 1994. Significant historical developments in thermal methods for measuring sap flow in trees. Agric. Forest Meteorol. 72, 113–132.

Swanson, R.H., Whitfield, D.W.A., 1981. A numerical analysis of heat pulse velocity and theory. J. Exp. Bot. 32, 221–239.

Viewig, G.H., Ziegler, H., 1960. Thermoelektrische Registrierung der Geswindigkeit des Transpirationsstromes I. Ber. Deutsche Bot. Ges. 73, 221–226.